# Assembly of metabolons in yeast using Cas6-mediated RNA scaffolding

# Anhuy Pham<sup>1</sup>, Shane Bassett<sup>1</sup>, Wilfred Chen<sup>2</sup>, and Nancy A. Da Silva<sup>1\*</sup>

<sup>1</sup> Department of Chemical and Biomolecular Engineering University of California, Irvine, CA, USA 92697-2580

\*Corresponding author

**Tel:** (+1)949-824-8288

E-mail: ndasilva@uci.edu

<sup>&</sup>lt;sup>2</sup> Department of Chemical and Biomolecular Engineering University of Delaware, Newark, DE, USA 19716

#### **ABSTRACT**

Cells often localize pathway enzymes in close proximity to reduce substrate loss via diffusion and to ensure carbon flux is directed toward the desired product. To emulate this strategy for the biosynthesis of heterologous products in yeast, we have taken advantage of the highly specific Cas6-RNA interaction and the predictability of RNA hybridizations to demonstrate Cas6mediated RNA-guided protein assembly within the yeast cytosol. The feasibility of this synthetic scaffolding technique for protein localization was first demonstrated using a split luciferase reporter system with each part fused to a different Cas6 protein. In Saccharomyces cerevisiae, luminescence signal increased 3.6- to 20-fold when the functional RNA scaffold was also expressed. Expression of a trigger RNA, designed to prevent formation of a functional scaffold by strand displacement, decreased the luminescence signal by nearly 2.3-fold. Temporal control was also possible, with induction of scaffold expression resulting in an up to 11.6-fold increase in luminescence after 23 h. Cas6-mediated assembly was applied to create a two-enzyme metabolon to redirect a branch of the violacein biosynthesis pathway. Localizing VioC-VioE together increased the amount of deoxyviolacein (desired) relative to prodeoxyviolacein (undesired) by 2fold. To assess the generality of this colocalization method in other yeast systems, the split luciferase reporter system was evaluated in Kluyveromyces marxianus; RNA scaffold expression resulted in an increase in luminescence signal of up to 1.9-fold. The simplicity and flexibility of the design suggest that this strategy can be used to create metabolons in a wide range of recombinant hosts of interest.

#### **Key Words:**

CRISPR-Cas6, Synthetic scaffold, RNA, Saccharomyces cerevisiae, Kluyveromyces marxianus, strand displacement

#### INTRODUCTION

The slow diffusion of intracellular molecules is a critical challenge for maintaining efficient cellular functions. To overcome this issue, cells have evolved to localize many of their metabolic pathways within intracellular organelles (such as compartmentalization of the TCA cycle within mitochondria) or to cluster their enzymes into functional metabolons for production of essential metabolites<sup>1,2</sup>. These strategies help the cells to improve catalytic efficiency, mitigate kinetic constraints, relieve the effects of toxic intermediates, lower the chances of substrate competition, and provide a means for quick shifts in desired product formation in response to external stimuli<sup>1</sup>. To emulate natural cell strategies, there is significant interest in colocalizing enzymes in organelles or constructing cytosolic synthetic metabolons for efficient channeling of substrates to desired products<sup>3,4</sup>.

The most straightforward approach to create cytosolic metabolons has involved fusing two proteins to catalyze successive reactions<sup>5,6</sup>. An alternate strategy for protein scaffolding entailed fusing interaction domains from metazoan signaling proteins to control metabolon assembly and modulate metabolic flux in *Escherichia coli*<sup>7</sup> and *Saccharomyces cerevisiae*<sup>8</sup>. These scaffolding technologies have proven successful for mediating synthetic metabolon assembly and improving product titers in bacteria,<sup>9,10</sup> but can face challenges in eukaryotes. In yeast, special attention is needed in the selection of protein-ligand interactions for protein scaffold assembly due to the possibility of cross-talk with native yeast proteins, which reduces scaffolding efficiency<sup>11</sup>. While a number of strategies for enzyme colocalization have been successful in the yeast cytosol<sup>12</sup>, ranging from scaffolds (such as cohesin and dockerin<sup>13,14</sup>, affibodies and anti-idiotypic affibodies<sup>15</sup>) to targeting the surface of the endoplasmic reticulum (ER)<sup>16</sup>, many lack dynamic controllability. This becomes an issue when the introduced pathway is deleterious to native

functions or when a product is toxic to the host, given the automatic and irreversible nature of these colocalization strategies. To circumvent such concerns, Zhao et al.<sup>17</sup> demonstrated the use of a dynamic, light inducible system for creating synthetic enzyme clusters in yeast to direct carbon flux toward the desired product, resulting in a 6-fold increase in product formation and 18-fold increase in product specificity.

Nucleic acids, particularly DNA, have also been implemented as artificial scaffolds for enzyme assembly due to their well-defined interactions, the existence of a large number of natural DNA-binding proteins, and generally high stability<sup>18,19</sup>. Several studies have successfully utilized DNA constructs to form artificial scaffolds to increase desired product titers<sup>20–23</sup>; however, this strategy is not applicable in eukaryotes due to DNA localization in the nucleus. In yeast, the use of RNA as scaffolds is a more attractive alternative; they also possess a high affinity toward their protein partners<sup>24,25</sup> while being able to freely diffuse through the cytoplasm. Successful use of RNA as a synthetic scaffold *in vivo* has been shown in *E. coli*, demonstrating its ability to control the spatial organization of a hydrogen-producing pathway or to optimize pentadecane production<sup>26,27</sup>. Furthermore, RNA-RNA hybridizing interactions can be dynamically regulated via toehold-mediated strand displacement (TMSD), a mechanism which allows a single stranded RNA input to bind and dislodge an established RNA-RNA hybridized pair<sup>28,29</sup>.

As part of the bacterial CRISPR defense system, Cas6 proteins work by first recognizing and binding to specific RNA hairpin structures before cleaving at the 3' end, creating an RNA-Cas6 complex with unique 5' RNA handles<sup>30–32</sup>. Exploiting the high affinity of Cas6 to RNA substrates, stem loop recognition site specificity, and the ability of Cas6 to remain bound to RNA allows us to assemble Cas6-RNA heterodimers by RNA hybridization. The orthogonal Cas6 proteins can be targeted to distinct stem loops, and artificial complementary "guide" RNA handles

used for RNA-RNA hybridization. Fusing proteins of interest to our Cas6 orthologs thus creates a synthetic metabolon, localizing sequential pathway enzymes proximal to each other. Mitkas *et al.* successfully demonstrated Cas6-mediated RNA-guided protein assembly *in vitro* and then created a metabolon in *E. coli* to improve indole-3-acetic acid and malate production<sup>33</sup>. In each case, the two pathways enzymes were fused to the Cas6 orthologs Csy4 from *Pseudomonas aeruginosa*<sup>31</sup> and the native *E. coli* Cse3<sup>34</sup>.

This approach would be of great value for the creation of small synthetic metabolons in eukaryotic cells, especially yeast. The highly specific interaction between the different orthologs of Cas6 and their RNA binding sites, along with the predictability of RNA-RNA hybridization ensures that such a system would have minimal crosstalk with the endogenous processes within the yeast. Furthermore, TMSD can be used to regulate both the association and dissociation of the RNA scaffolds, opening up the possibility of a fully dynamic control system. In this work, we constructed and evaluated this Cas6-mediated RNA-guided enzyme colocalization strategy in both *S. cerevisiae* and the non-conventional thermotolerant yeast *Kluyveromyces marxianus*. We demonstrated successful protein colocalization via reconstitution of a split luminescence reporter, and pathway redirection of a partial violacein pathway. We also showed the potential of TMSD for regulating RNA scaffold formation, and temporal control of scaffold assembly using an inducible promoter. To our knowledge, this is the first RNA-based protein assembly technique for enzyme colocalization in yeast.

#### RESULTS AND DISCUSSION

# Cas6-mediated RNA-guided protein colocalization in S. cerevisiae

To determine whether Cas6-mediated protein assembly is functional in S. cerevisiae, we first evaluated the ability to reconstitute a split luciferase. The NanoBiT® Split Luciferase reporter system from Promega utilizes an engineered NanoLuc® luciferase comprised of two small separate subunits (LgBiT [18 kDa] and SmBiT [1.3 kDa]) that can be easily fused to proteins without interfering with their functions. This luciferase is only fully functional and capable of emitting a luminescence signal if the two subunits are in close proximity<sup>35,36</sup>. LgBiT and SmBiT were C-terminally fused to the Cas6 orthologs Csy4 and Cse3, respectively, using a short flexible GGGGS linker. Both of the gene fusion constructs were placed under the transcriptional control of the galactose-inducible GAL1 promoter (Figure S1) and integrated into S. cerevisiae strain BY4741 at chromosomal sites XI-5 and XI-3<sup>37</sup>, respectively, creating strain BY GALnbit. The RNA transcript encoding the scaffold (Figure S2A) was inserted under the control of tRNA Phe (an RNA polymerase III promoter) and upstream of an HDV ribozyme and the SNR52 terminator<sup>38</sup> to minimize the effects of post-transcriptional modifications on our synthetic RNA scaffolds and allow proper folding. This single RNA transcript containing specific binding sequences for Cse3 and Csy4, along with two complementary 5' handles and a distinct toehold for future manipulation of the RNA scaffold, was expressed from a multi-copy 2µ plasmid (Binding scaffold plasmid) (Figure S2A, Table S3).

To examine whether our RNA scaffolds could guide Cas6-mediated luciferase reconstitution in the yeast cytosol (Figure 1A), BY\_GALnbit carrying the Binding scaffold plasmid was cultivated for 28 h in 2% galactose medium to induce expression of Cse3-SmBiT and Csy4-LgBiT; this was followed by harvest and luminescence measurements. As controls,

BY GALnbit was also transformed with an Empty plasmid containing no RNA transcript, and a plasmid containing a scrambled RNA transcript that would prevent RNA hybridization (Figure S2B). The Empty plasmid control resulted in a nonnegligible basal specific luminescence (Figure 1B). This is likely due to the fused proteins being under the control of the strong GAL1 promoter<sup>39,40</sup>; when Cse3-SmBiT and Csy4-LgBiT are expressed in abundance, the chance of random reconstitution in the cytoplasm increases. However, when Cse3-SmBiT and Csy4-LgBiT were expressed in tandem with the Binding scaffold, specific luminescence increased 3.6-fold relative to the basal level, demonstrating the ability of these RNA scaffolds to colocalize the two luciferase subunits. As expected, the specific luminescence using the Scrambled scaffold was approximately 1.9-fold lower than with the Binding scaffold. Interestingly, the use of the Scrambled scaffold resulted in a slightly higher luminescence than with the Empty plasmid. This may be due to luminescence when Cse3-SmBit and Csy4-LgBit bind to their respective hairpins on the same RNA transcript before the Cas6 orthologs have the opportunity to cut the strand. To confirm this, we performed RT-qPCR using strains BY4741 and BY GALnbit both expressing the Scrambled scaffold plasmid; only the latter strain expresses the Cas 6 proteins. The full RNA transcript for BY GALnbit was approximately 3.2-fold lower relative to BY4741 (Figure S3), consistent with proper Cas6-mediated RNA processing. However, full-length, uncleaved RNA was still detectable. Thus, not all of the RNA is processed, consistent with the higher luminescence observed for BY GALnbit expressing the Scrambled scaffold RNA.

The scaffold:protein ratio has been found to be extremely important for colocalization strategies<sup>12</sup>. This ratio is important in the current work; a low amount of RNA transcript would be insufficient to bind all expressed Cas6 orthologs while too much RNA transcript would increase the number of scaffolds with only one protein (Cse3-SmBiT or Csy4-LgBiT) bound. We thus also

expressed the scaffold from low copy CEN/ARS plasmids. As expected, the same trend was observed, with the specific luminescence in the strain expressing the Binding scaffold approximately 3-fold higher (p < 0.01) relative to the Scrambled scaffold (Figure S4). However, specific luminescence was approximately 70% higher when scaffold expression was from  $2\mu$  plasmids (Figure 1B). This indicates that increasing the amount of total RNA transcripts increases colocalization of the two proteins. We thus continued expressing the RNA scaffolds from the higher copy  $2\mu$  plasmids.

To determine whether TMSD can be used to dynamically regulate interactions between the RNA handles, an additional RNA feature encoding a trigger RNA that shares greater complementarity to one of the gRNA handles was added to the RNA construct (Figure S2C, Table S3), creating the Trigger scaffold. After RNA processing by the two Cas6 orthologs, the Csy4 gRNA handle can hybridize with the Trigger scaffold rather than the Cse3 gRNA. The Trigger scaffold displaces the Cse3 gRNA handle and prevents reconstitution of a functional luciferase (Figure 1C). Based on our constructs (Figure S2C), competitive hybridization by the trigger may also occur. This new Trigger scaffold was expressed from 2µ plasmids in strain BY GALnbit. As a control, a Scrambled Trigger RNA, to prevent displacement of the Cse3 gRNA handle (Figure S2D), was similarly expressed. The use of the Trigger scaffold gave a specific luminescence signal similar to that of the Scrambled scaffold and 2.3-fold lower than that for the Binding scaffold (Figure 1B). This indicates that the Trigger successfully prevented the hybridization of the Cse3 and Csy4 gRNA handles, inhibiting luciferase reconstitution and resulting in a reduction in luminescence signal. In addition, the difference between Scrambled Trigger Binding scaffold and the Binding scaffold was not significant, indicating RNA hybridization was maintained between the two guide handles (Figure 1B). In this system, the Trigger was automatically generated via the cleaving of the RNA scaffold construct by the endoribonucleases rather than via induction of a separate transcript. Nonetheless, the results highlight how the additional toehold sequence can be utilized in yeast to induce TMSD, and the potential for dynamic control of protein colocalization.

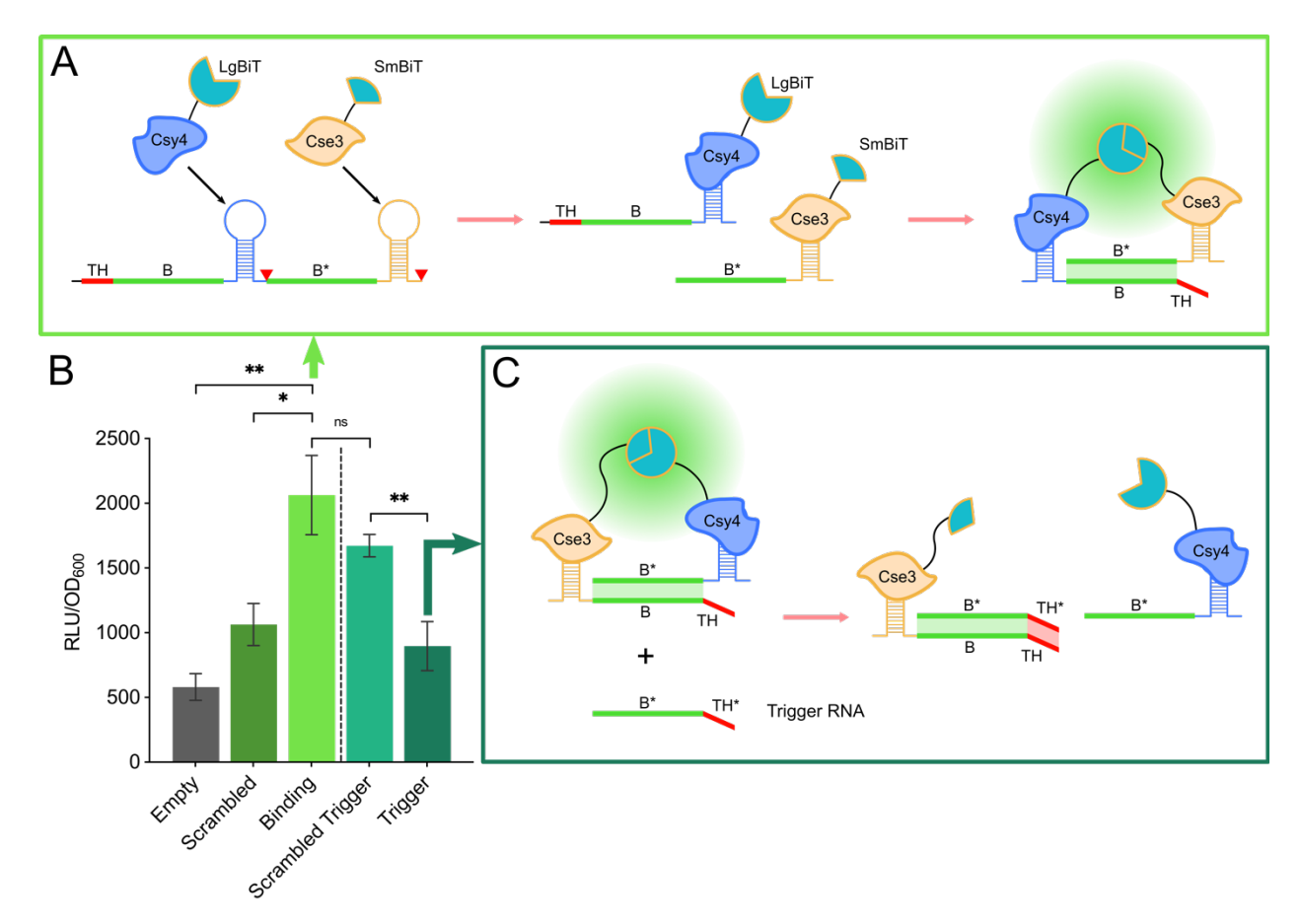


Figure 1. Cas6-mediated RNA-guided reconstitution of NanoBiT luciferase in S. cerevisiae.

(A) Two Cas6 orthologs fused to their respective SmBit or LgBiT subunits bind to their hairpin recognition structures, where Cas6 cleaves at the 3' end (red triangles) and forms a Cas6-RNA complex. The resulting mature crRNAs (B and B\*) hybridize with one another given their complementary sequences, bringing the two NanoBiT subunits in proximity for reconstitution. (B) Strains constitutively expressing the Binding RNA scaffold from high copy 2μ plasmids significantly improved specific luminescence over the basal level and a completely Scrambled scaffold. (C) Reconstituted NanoBiT can be disassembled using an additional RNA trigger (B\*-TH\*), designed to share greater complementarity with one of the mature crRNAs, via TMSD.

Expression of this RNA trigger reduced luminescence down to basal levels (B), indicative of NanoBiT disassembly. Bars represent the mean  $\pm$  one SEM, n = 6, \*p < 0.05, \*\*p < 0.01.

### Temporal control of Cas6-mediated protein colocalization via galactose induction

We next evaluated temporal control of protein assembly by placing expression of the RNA scaffold under the regulation of an inducible polymerase II promoter. To prevent post-transcriptional modifications (e.g., 5' cap and polyA tail) associated with RNA polymerase II transcription, we flanked the RNA scaffold transcript with hammerhead and HDV self-cleaving ribozymes<sup>41–43</sup> at the 5'- and 3'-ends, respectively. We tested three inducible promoters: *S. cerevisiae DDI2* promoter, *S. cerevisiae CUP1* promoter, and *S. cerevisiae GAL1* promoter. Among the three candidates, only the *GAL1* promoter was shown to reliably induce RNA transcript expression under conditions that did not interfere with the luminescence assay. To decouple protein and scaffold expression, we replaced the *GAL1* promoters in the Cse3-SmBiT and Csy4-LgBiT expression cassettes with the strong constitutive *TEF1* promoter. These new cassettes were again integrated into *S. cerevisiae* BY4741 at chromosomal sites XI-3 and XI-5, respectively, to create strain BY TEFnbit.

To first confirm our protein fusions were adequately expressed from the *TEF1* promoter, BY\_TEFnbit was transformed with the original RNAP III scaffold plasmids and then cultivated for 25 h in 2% dextrose medium before harvest and luminescence measurements. The combination of Cse3-SmBiT and Csy4-LgBiT (*TEF1* promoter) and expression of the Binding scaffold was successful with a luminescence signal 7.2-fold higher than that of the Scrambled scaffold, and nearly 20-fold higher than the Empty plasmid (Figure 2A). Again, the luminescence signal in strains expressing the Scrambled scaffold was repeatedly slightly higher than that of the Empty plasmid control, suggesting that some of the fusion proteins bind and emit a luminescence signal

before the RNA transcript is cleaved. To assess the stability of these RNA scaffolds with time for protein colocalization, we repeated the study harvesting after 42 h (late stationary phase). Although the luminescence signal significantly decreased between 25 and 42 h, the strain expressing the Binding scaffold still maintained a higher specific luminescence relative to the two controls, with a 4.6- and 6.4-fold increase over the Scrambled scaffold and Empty plasmid, respectively (Figure 2B). Thus, the scaffolds were still able to colocalize the two luciferase subunits and produce substantially higher luminescence signals than the two controls, demonstrating function at late time points.

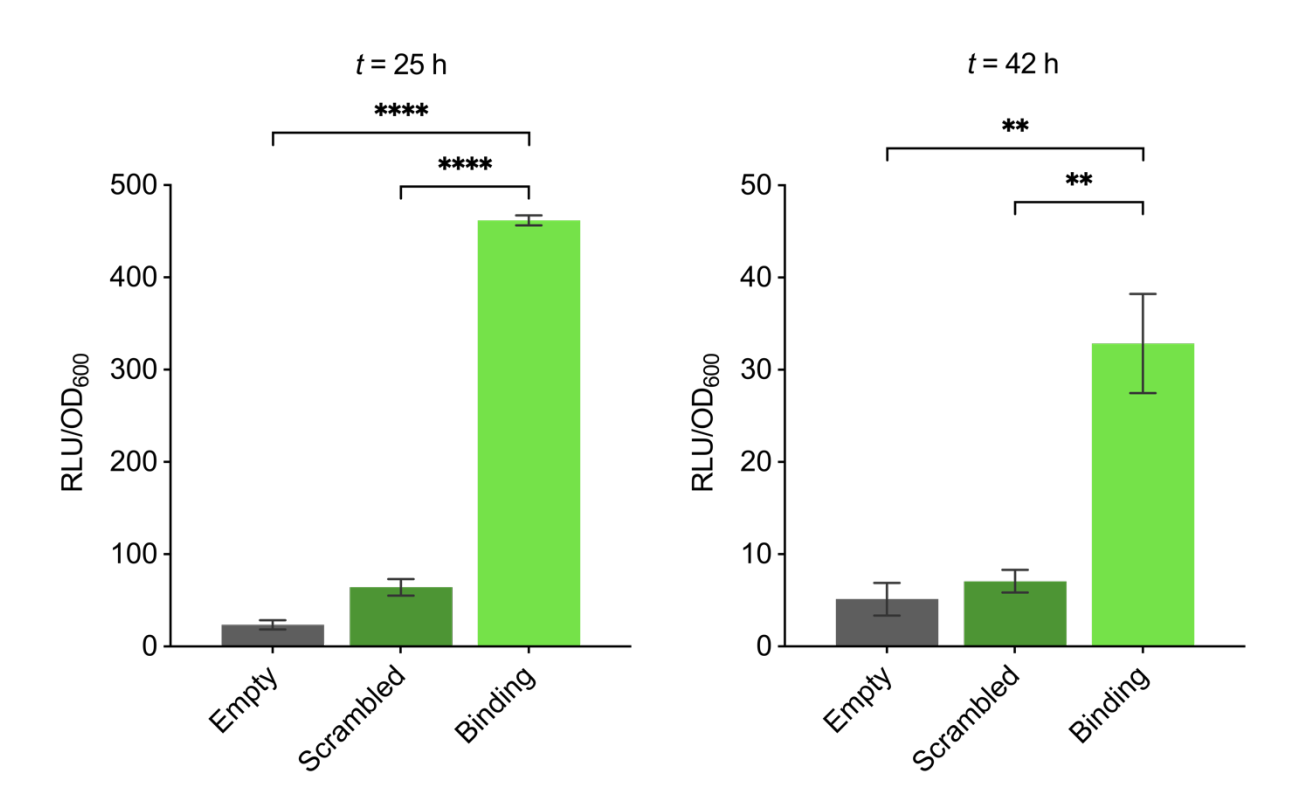


**Figure 2. Luminescence over time with constitutive** *TEF1* **promoter-driven protein expression.** Specific luminescence was recorded at (A) 25 h and (B) 42 h post-inoculation from *S. cerevisiae* strains expressing integrated Cas6-NanoBiT subunit fusions from the strong constitutive *TEF1* promoter, and RNA scaffolding transcripts from a constitutive RNAP III tRNA promoter on multi-copy 2μ plasmids. Binding scaffold significantly improved NanoBiT

reconstitution and demonstrates functionality for protein colocalization well into stationary phase. Bars represent the mean  $\pm$  one SEM, n = 4, \*\*p < 0.01, \*\*\*\*p < 0.0001.

To demonstrate that Cas6-mediated RNA-guided protein assembly can be temporally controlled via external stimuli, we tested scaffold expression using galactose induction. We transformed strain BY TEFnbit with the new Binding and Empty plasmids under the RNAP II GAL1 promoter. To allow induction, we first cultured these strains in 2% raffinose medium to avoid glucose repression of the GAL1 promoter. After 25 h, the cultures were centrifuged, the medium discarded, and the cultures resuspended in either 4% raffinose (uninduced) or 4% galactose media (to induce the expression of the Binding scaffold) (Figure 3A). Despite being cultured in different sugar sources, no significant difference in cell growth was observed between different groups at the time of harvest (Figure S5). Prior work has shown that induction of the GAL1 promoter does not peak until more than 10 hours after induction<sup>39</sup>. As expected, no increase in luminescence was observed 2 h following the induction of RNA scaffold; at 6 hours, luminescence increased, but the difference was still small (Figure S6). Therefore, we performed the luminescence assay at either 9 or 23 hours after induction to ensure that enough scaffold RNA was generated. As expected, both the Binding scaffold in raffinose (uninduced) and the Empty plasmid showed a similar basal specific luminescence level, whereas the Binding scaffold in galactose (induced) had a specific luminescence signal 3- and 11.6-fold higher after 9 h and 23 h of induction, respectively (Figures 3B, C). Interestingly, while the specific luminescence signal from the induced Binding scaffold remained at approximately the same level after both induction time points, the specific luminescence from both Empty plasmid and non-induced Binding scaffold experienced a marked decrease over the additional 14 h induction period. This likely indicates a drop in protein level and thus random reconstitution in the absence of scaffold. It also showed that the quantity of RNA scaffold was most likely the limiting factor. Overall, the results demonstrate that our Cas6-mediated enzyme colocalization strategy can be controlled by an external stimulus in *S. cerevisiae*.

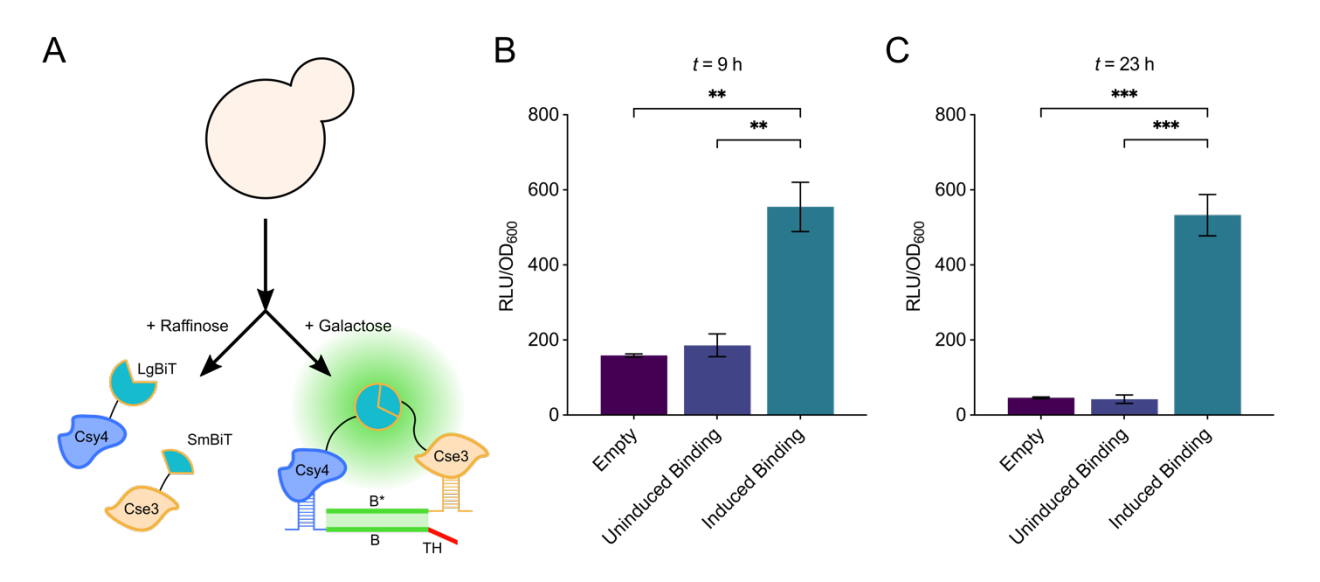


Figure 3. Temporal control of Cas6-mediated RNA-guided NanoBiT reconstitution through galactose induction. (A) *S. cerevisiae* strain BY\_TEFnbit, constitutively expressing Cas6-NanoBiT subunit fusions, expressing the Binding scaffold under the inducible RNAP II *GAL1* promoter. Cells were grown in galactose for 24 hour and then transferred to either raffinose (no induction) or galactose (fully induced) medium. Specific luminescence was measured for strains harboring no transcript (Empty), Binding transcript (in raffinose), or Binding transcript (in galactose at (B) 9 h and (C) 23 h post-induction. Bars represent the mean  $\pm$  one SEM, n = 3, \*\*p < 0.001, \*\*\*p < 0.001.

# Utilizing Cas6-mediated protein colocalization for pathway redirection in S. cerevisiae

We next evaluated the use of this colocalization strategy for metabolon assembly and carbon flux redirection in *S. cerevisiae*. The violacein pathway is a 5-enzyme multi-branch pathway native to *Chromobacterium violaceum* that feeds from L-tryptophan biosynthesis and results in different colored products depending on the substrate channeling order<sup>44</sup>. Here, we chose

to use one of the branches, consisting of four of the five enzymes (VioA, VioB, VioE, and VioC), for pathway redirection away from prodeoxyviolacein (PDV; undesired) and toward deoxyviolacein (DV; desired) (Figure 4A).

The VioA and VioB genes were integrated into the *S. cerevisiae* BY4741 genome under the control of the *TEF1* promoter at sites XI-3 and XI-5, respectively, resulting in strain BY\_VioAB. The subsequent two proteins, VioE and VioC, were C-terminally fused to Cse3 and Csy4, respectively, again via a GGGGS linker. The gene fusions encoding Cse3-VioE and Csy4-VioC were also placed under *TEF1* promoter control and integrated into BY\_VioAB at sites X-2 and XII-4<sup>37</sup>, respectively, creating strain BY\_VioAB3E4C. VioA and VioB will thus be free-floating, while VioE and VioC can bind to the RNA scaffold via their respective Cas6 orthologs to form a 2-enzyme metabolon (Figure 4B). Strain BY\_VioAB3E4C was transformed with the original RNAP III 2μ plasmid system containing either the Binding scaffold or no RNA transcript. The strains were cultured for 24 h in 2% dextrose media, harvested, and the extracellular products quantified via HPLC. Initial testing revealed no significant difference in the ratio DV/Total Products in the strain expressing the Binding scaffold (Figure S7). This is likely due to RNA scaffold limitation, as scaffold was found to be limiting in our luminescence studies above.

To increase the ratio of RNA scaffold to Cas6 proteins, we truncated the promoter of the *URA3* selection marker on the scaffold plasmid. This strategy has been reported to force cells to maintain a higher plasmid copy number<sup>45–47</sup>. The Binding, Scrambled, and no RNA control scaffold cassettes were cloned onto this new plasmid and transformed into strain BY\_VioAB3E4C. The strains were then cultured in 2% dextrose media for 24 hours, after which the violacein products were quantified via HPLC. The absolute titer of the desired DV increased 1.8- and 2.2-fold for the Binding scaffold relative to the Empty plasmid and Scrambled scaffold controls,

respectively (Figure 4C), while the titer of the undesired PDV decreased 20% and 34% relative to these controls. Similarly, DV/PDV selectivity increased 2- and 2.6-fold for the Binding scaffold relative to the Empty plasmid and Scrambled scaffold controls, respectively (Figure 4D). The strains expressing the Binding scaffold had a larger variation in product titer, possibly due to the variation in copy number of the ultra-high copy plasmid and further demonstrating the strong dependence of the system on the protein:scaffold ratio within the cells. These results conclusively demonstrate that our Cas6-mediated RNA-guided colocalization strategy can be used for functional enzyme metabolon assembly in the cytosol of *S. cerevisiae*, enabling substrate channeling and allowing pathway redirection.

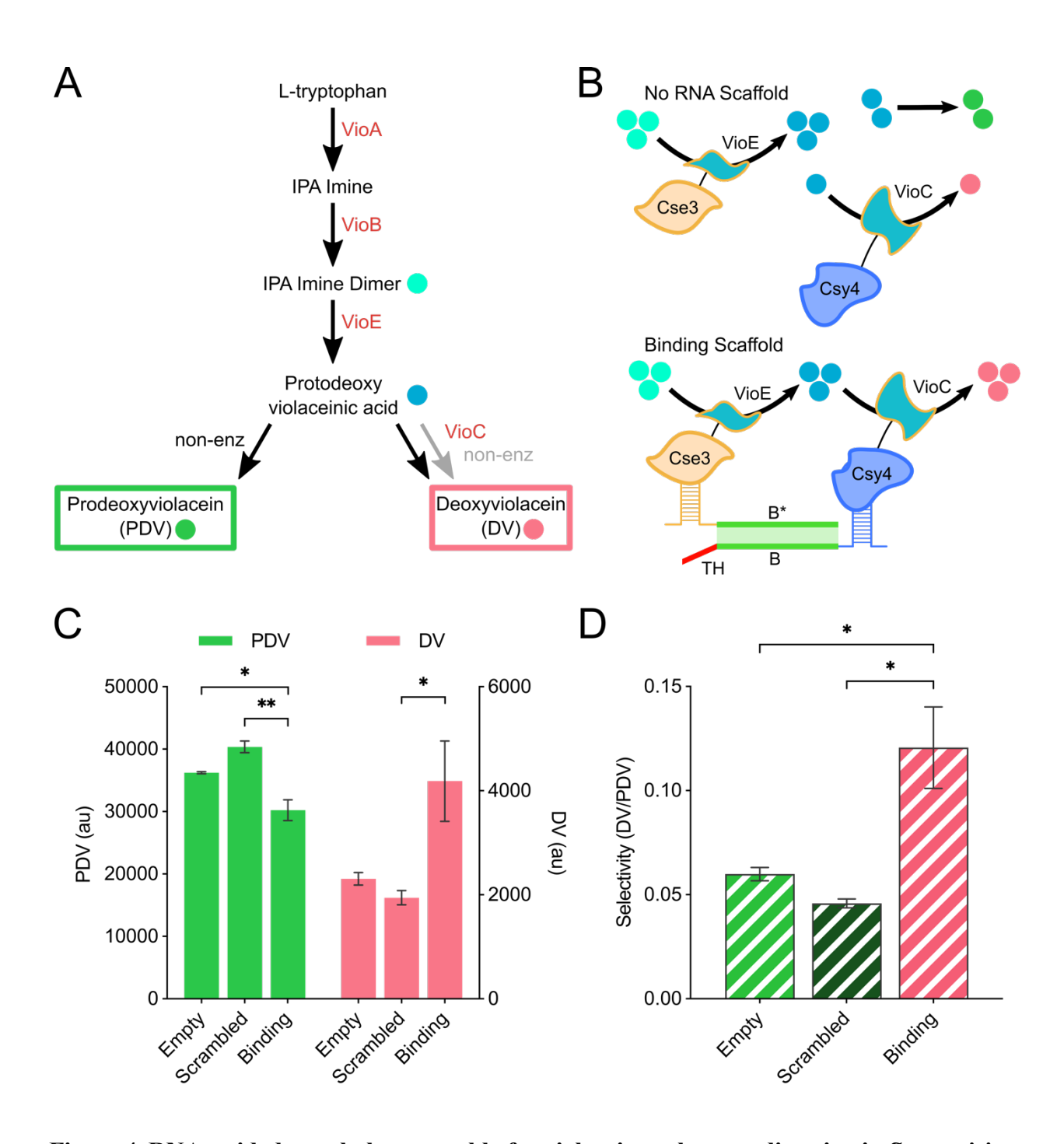


Figure 4. RNA-guided metabolon assembly for violacein pathway redirection in S. cerevisiae.

(A) In the partial violacein pathway, the amino acid L-tryptophan is converted to protodeoxyviolaceinic acid (PDVA) via the enzymes VioA, VioB, and VioE. A subsequent non-enzymatic reaction can then convert the PDVA to PDV, or the enzyme VioC can convert the PDVA to an intermediate which is then non-enzymatically converted to DV (gray arrow). (B) VioA, VioB, VioC, VioE were integrated into the chromosomes, with VioE and VioC expressed

as C-terminal fusions to Cse3 and Csy4, respectively. When no RNA scaffold is expressed, PDV formation should be favored; expression of the Binding scaffold should favor DV formation. (C) Titers for PDV (undesired) significantly decrease for the Binding scaffold relative to both the Empty plasmid and Scrambled scaffold controls, while DV (desired) titers simultaneously increase. (D) Desired to undesired product selectivity also increased with the Binding scaffold, indicating successful metabolon assembly and violacein pathway redirection. Bars represent the mean  $\pm$  one SEM, n = 3, \*p < 0.05, \*\*p < 0.01.

# Characterizing Cas6-mediated protein colocalization in K. marxianus

We next investigated whether the Cas6-mediated enzyme assembly strategy could be extended to other yeast systems. The non-conventional thermotolerant yeast *K. marxianus* has garnered much attention in recent years as a microbial powerhouse. Because of its thermal<sup>48</sup> and acid tolerance<sup>49</sup>, rapid growth rate (twice that of *S. cerevisiae*)<sup>50</sup>, and ability to consume a wide range of carbon sources<sup>51–53</sup> this yeast holds great potential for industrial biomanufacturing. Recent advances in strain engineering methods have propelled *K. marxianus* forward, and the establishment of an intracellular enzyme scaffolding system in this yeast would be an important addition to the synthetic biology toolbox. We thus adapted our Cas6-mediated RNA-guided colocalization system for use in *K. marxianus* and evaluated the ability of the RNA-bound Cas6 orthologs to reconstitute the NanoBiT® Split Luciferase protein pair, LgBiT and SmBiT, similar to our studies in *S. cerevisiae*.

We initially expressed the Cas6-NanoBiT protein pairs and RNA transcripts from twoplasmid systems, with one plasmid expressing the RNA transcripts and the other expressing the Cas6 protein fusions. The two plasmids were either both low copy *K. marxianus* CEN/ARS or both higher copy *K. lactis* pKD1<sup>51</sup> plasmids. LgBiT and SmBiT were fused C-terminally to Csy4 and Cse3 respectively (the same constructs as for *S. cerevisiae* above) and expressed using the *S. cerevisiae GAL1* promoter and *CYC1* terminator as a single coding sequence, separated by a T2A "self-cleaving" peptide sequence (Figure 5A). These and other 2A peptide sequences while called "self-cleaving" act through a ribosomal skipping mechanism<sup>54</sup> and have been used for polycistronic expression of proteins from a single coding unit in eukaryotes (Figure S8). Plasmid pairs were co-transformed into *K. marxianus* strain CBS712 $\Delta U\Delta L$ , cultured overnight at 37°C in selective glucose media, inoculated for expression in selective galactose media and cultured for 15 h at 37°C before harvesting and luminescence measurements.

Expression of both RNA and protein fusions from low-copy plasmids resulted in a 1.5- and 2.4-fold increase in specific luminescence for the Binding scaffold relative to the Empty plasmid and Scrambled scaffold controls, respectively (Figure 5B: LP+LR). This demonstrates both the correct recognition of the RNA stem loop handles by their respective Cas6 orthologs in *K. marxianus* and RNA-mediated hybridization of the two Cas6-RNA complexes. This also indicates endoRNAse activity of both the *E. coli* Cse3 and the *P. aeruginosa* Csy4 in this yeast. For the two multi-copy pKD1 plasmids (Figure 5B: HP+HR), overall luminescence was more than 2-fold higher relative to that measured for the CEN/ARS plasmids. Signal from the Binding scaffold was 1.9-fold higher than basal luminescence, and 1.3-fold higher than luminescence from the Scrambled scaffold. A higher luminescence was observed for the Scrambled scaffold relative to the Empty plasmid when the higher copy pKD1 plasmids were used, similar to what was observed in *S. cerevisiae*. Again, this could be due to luciferase reconstitution prior to Cas6 processing of the RNA scaffolds.

To further optimize this system and eliminate plasmid stability issues that may arise from carrying and propagating two plasmids, we integrated the Cas6-NanoBiT cassette into the

CBS712 $\Delta U\Delta L\Delta K$  genome<sup>55</sup>. This keeps RNA scaffold levels high relative to Cas6-fused protein levels (as was found to be important in *S. cerevisiae*). With this system, we observed a 1.5- and a 1.7-fold increase in specific luminescence relative to the two controls (Figure 5B: IP+HR). From these results, we can conclude that only low copy expression of the proteins is needed. In addition to demonstrating that the Cas6 orthologs are functional in this non-conventional yeast, the results show that the single, bicistronic cassette with the T2A peptide was successful for expressing the two Cas6-NanoBiT subunits; the T2A peptide has been shown to work *S. cerevisiae*<sup>56</sup> but not previously in *K. marxianus*. Most importantly, RNA-guided reconstitution of the NanoBiT® Split Luciferase demonstrates that this protein colocalization strategy was readily translatable to another yeast species.

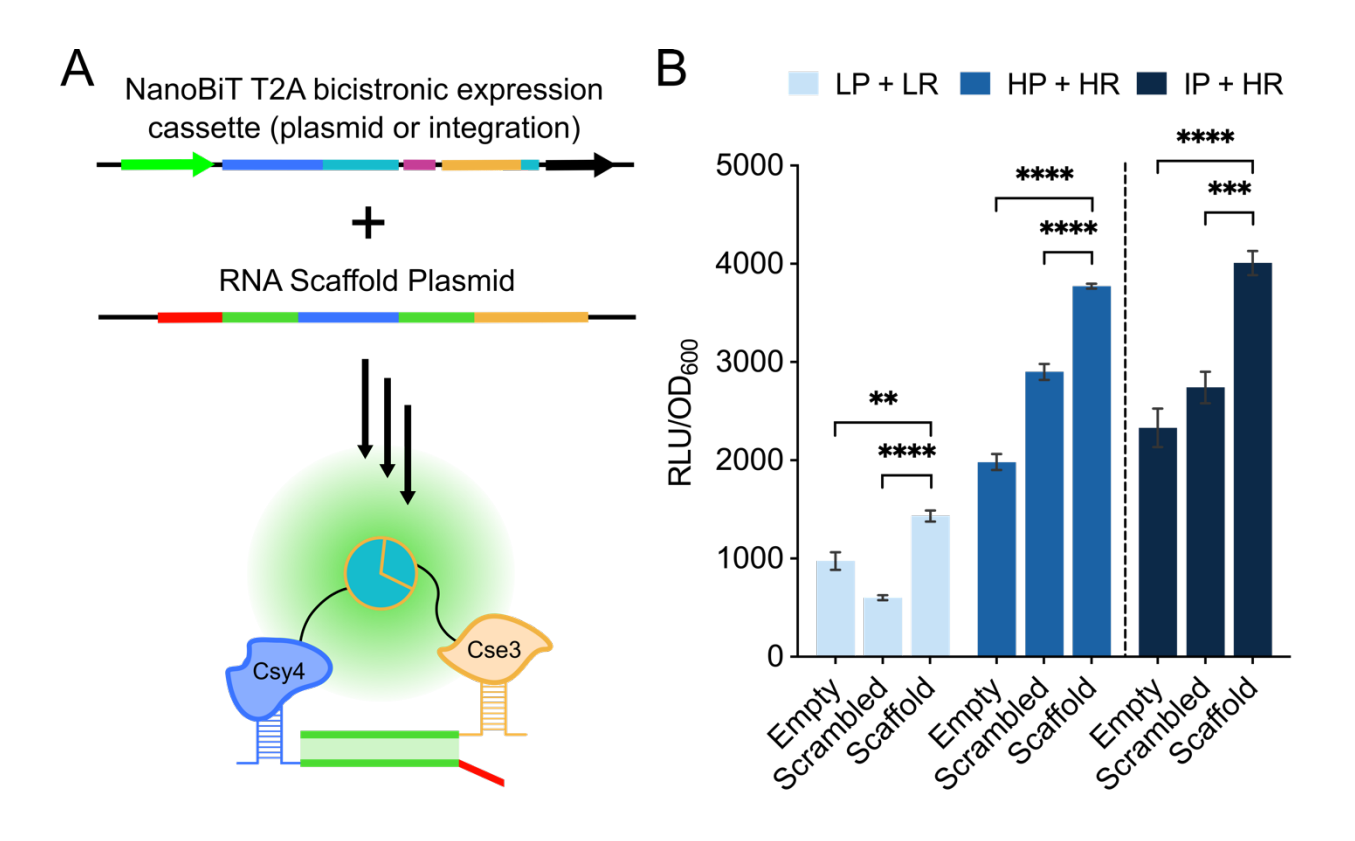


**Figure 5. RNA-guided reconstitution of NanoBiT luciferase in K. marxianus.** (A) Cse3-SmBiT and Csy4-LgBiT were expressed using the *S. cerevisiae GAL1* promoter from a single gene

cassette including a T2A self-cleaving peptide sequence (pink bar) on low or multi-copy K. marxianus plasmid pairs or through chromosomal integration. (B) Specific luminescence was measured after 15 h for strains harboring an Empty plasmid without any scaffold for basal luminescence, a Scrambled scaffold as the negative control, and a Binding scaffold for NanoBiT reconstitution. LP + LR: low copy protein plasmid, low copy RNA plasmid; HP + HR: high copy protein plasmid, high copy RNA plasmid; IP + HR: integrated proteins, high copy RNA plasmid. Bars represent the mean  $\pm$  one SEM, n = 5, \*\*\*p < 0.001, \*\*\*\*p < 0.0001.

#### **CONCLUSIONS:**

Enzyme colocalization in yeasts via synthetic constructs and organelle targeting have attracted great interest as a strategy to overcome bottlenecks in biosynthesis of desired products while minimizing the effects of toxic intermediates<sup>3,12</sup>. Here, we demonstrated the use of Cas6mediated RNA-guided protein scaffolding as an efficient means of protein colocalization in the yeast cytosol. We successfully demonstrated reconstitution of the subunits of a split luciferase, allowing several-fold higher luminescence signals upon scaffold binding in S. cerevisiae. Switching our RNA cassette from an RNAP III promoter to the galactose inducible *GAL1* promoter gave us temporal control over protein assembly, leading to up to an 11.6-fold increase in measurable luminescence following galactose induction. This strategy was also successful for metabolon assembly; cascading two of the four violacein proteins from the proviolacein pathway redirected pathway flux towards the desired product with an approximate two-fold increase in the desired versus undesired product. Finally, this colocalization strategy was shown to be functional in K. marxianus, suggesting that it may be broadly applicable in other non-conventional yeasts. The research demonstrates for the first time that a synthetic RNA scaffold can be used to colocalize proteins in the yeast cytosol, providing a new synthetic biology tool for controlling protein localization in yeast. Continuing optimization and extension to multi-enzyme constructs will further expand the applications of this Cas6-mediated RNA-guided protein scaffold.

#### **METHODS:**

#### Strain and Plasmid Construction

All plasmids and strains used in this work are listed in Table S1 with primers (and their applications) summarized in Table S2. All DNA sequences (e.g., for the scaffolds) are tabulated in Table S3. Primers were synthesized by Integrated DNA Technologies (IDT). PCR reactions were performed using Q5® Hot Start High-Fidelity DNA Polymerase from New England Biolabs (NEB, Ipswich, MA) and 2X PrimeSTAR® Max DNA Polymerase from Takara Bio, Inc (Kusatsu, Shiga, Japan). Gibson assembly reactions were performed using the NEBuilder® HiFi DNA Assembly Master Mix from NEB. All restriction enzymes and T4 DNA Ligase were purchased from NEB. All plasmids were confirmed by Sanger sequencing (Azenta Life Sciences, South Plainfield, NJ) prior to transformation into *S. cerevisiae* or *K. marxianus*.

Gibson Assembly was used for plasmid cloning, unless specified otherwise. To create pXP822-Cas6-NanoBiT, the Cse3-SmBiT-T2A-Csy4-LgBiT fragment was amplified and cloned into the pXP822 backbone. To split Cse3-SmBiT and Csy4-LgBit into their individual gene expression cassettes, appropriate primer pairs were used to insert them into SpeI digested pXP822 and pXP821, respectively. To place the Cas6 fusion proteins under the *TEF1* promoter, the Cse3-SmBit and Csy4-Lgbit fragments were inserted into SpeI and XhoI digested pXP318. P2u-Cse3bCsy4b was created by inserting the Cse3bCsy4b fragment into the backbone generated from the sgRNA (2μ, *LEU2* marker) plasmid created from the Yeast Toolkit<sup>38</sup>. Trigger and ScrambledTrigger fragments were also cloned into the sgRNA backbone using the same set of

primers. Using p2u-Cse3bCsy4b as template, different sets of primers were used to create p2u-Binding and p2u-ScrambledBinding by Gibson Assembly. Both the ScrambledBinding and ScrambledTrigger was designed by randomly scrambled one of the hybridizing regions of the scaffold and then ensuring there is minimal interaction between the two via NUPACK web application<sup>57</sup>. Appropriate sets of primers and Gibson Assembly were used to switch the  $2\mu$  for the CEN/ARS fragment to create pCA-Binding and pCA-ScrambledBinding. HH-HDV fragments were created by amplifying two primers to create a double strand DNA before inserting into pXP821. Sets of primers were used to remove the LEU2 marker from p2u-Binding and p2u-ScrambledBinding and replace it with URA3 marker to create p2u-BindingURA3 and p2u-ScrambledBindingURA3. The Binding scaffold and Scrambled scaffold fragments were cloned into pCRCT plasmid backbone<sup>47</sup> to create p2u-BindingURA3t ScrambledBindingURA3t. Primers were used to linearize pXP318-Cse3-SmBiT and pXP318-Csy4-LgBiT and remove the SmBiT and LgBiT fragments. The VioE and VioC genes<sup>58</sup> were then cloned into the linearized fragments to create pXP318-csy4-VioC and pXP318-cse3-VioE.

For plasmid expression of Cas6-NanoBiT protein fusions in *K. marxianus*, plasmid pXP822-Cas6-NanoBiT was linearized by *EcoRI* to remove the *S. cerevisiae* 2μ origin and was ligated with the *EcoRI* digested *K. marxianus* CEN/ARS sequence from pCA-A<sup>51</sup> to create pKmCA-Cas6-NanoBiT. For high copy expression of these proteins, pXP22-Cas6-NanoBiT was PCR amplified to remove the 2μ origin (primers pKD1\_Cas6\_F and pKD1\_Cas6\_R) and Gibson assembled with the pKD1 high copy origin from *K. lactis* digested from pKD-A<sup>51</sup> at *SphI* to create pKD-Cas6-NanoBiT. RNA scaffolding plasmids, containing the AmpR-ColE1 ampicillin resistance-*E. coli* origin, *S. cerevisiae LEU2* marker, 2μ origin, and the tRNA<sup>Phe</sup> gene as a RNAP III promoter and the synthetic scaffolding sequence (Binding, Scrambled, or Empty), were adapted

to *K. marxianus* compatible plasmids by PCR amplifying each plasmid to remove the 2μ origin and Gibson assembled with the *EcoRI* digested *K. marxianus* CEN/ARS sequence from pCA-A or the *SphI* digested *K. lactic* pKD1 high copy origin from pKD-A, for a total of 6 scaffolding plasmids for expression in *K. marxianus*.

CRISPR-Cas9 was used to integrate the gene cassettes into the yeast genomes and all gene disruptions and integrations were verified by Sanger sequencing (Azenta Life Sciences, South Plainfield, NJ). In *S. cerevisiae*, the CRISPR-Cas9 system consisted of two plasmids: a low copy plasmid expressing Cas9 proteins and a high copy plasmid expressing gRNA plasmids<sup>59</sup>. Donors fragments were generated via PCR, using primers containing at least 40bps homology with the yeast genomes. *S. cerevisiae* strain BY\_GALnbit was created from BY4741 using donors amplified from pXP822-Cse3-SmBiT and pXP821-Csy4-LgBiT targeting site XI-3 and XI-5<sup>37</sup>, respectively. BY\_TEFnbit was created from BY4741 using donors amplified from pXP318-Cse3-SmBiT and pXP318-Csy4-LgBiT targeting site XI-3 and XI-5, respectively. BY4741VioAB was previously created in the lab by integrating donor generated from TEF1p-VioA-CYC1t and TEF1p-VioB-CYC1t into sites XI-3 and XI-5<sup>60</sup>. Donor fragments amplified from pXP318-cse3-VioE and pXP318-csy4-VioC were integrated into strain BYVioAB at site X-2 and XII-4<sup>37</sup> to create strain BYVioAB3E4C.

*K. marxianus* strains CBS712Δ*U*Δ*L* and CBS712Δ*U*Δ*L*Δ*K* were created from strains CBS712Δ*U*51 and CBS712Δ*U*Δ*K*55, respectively, by Cas9 targeting and disruption of the native *LEU2* locus using a 200 bp internally truncated *LEU2* gene as the donor55. Strain CBS712Δ*ULK-Cas6NanoBiT* was created by integrating the GAL1p-Cse3-SmBit-T2A-Csy4-LgBiT-CYC1t cassette at the Chr.IV-2 (IV-2) noncoding site<sup>61</sup>. Plasmids pDBtgr-Cas9-*LEU2* and pDBtgr-Cas9-14, both single-plasmid Cas9 systems harboring a cassette for Cas9 expression and an RNA RNAP

II cassette for gRNA expression<sup>55</sup>, was used for targeting the *LEU2* locus and IV-2 site, respectively. The full GAL1p-Cse3-SmBit-T2A-Csy4-LgBiT-CYC1t cassette was PCR amplified from pXP822-Cas6-NanoBiT and acted as donor sequence.

#### Media & Cultivation

Escherichia coli strains XL-1 Blue and DH5α were cultivated in 5 mL of lysogeny broth (LB) containing 150 μg/mL of ampicillin for molecular cloning and plasmid maintenance. All cultures were grown in 15 × 125 mm borosilicate culture tubes containing 3 mL of appropriate media and shaking at 250 rpm, unless otherwise specified. For plasmid transformation, yeasts were grown in YPD [10 g/L yeast extract (BD Difco<sup>TM</sup>), 20 g/L peptone (BD Difco<sup>TM</sup>), and 20 g/L D-glucose (Fisher Scientific)] at 30°C. Optical densities (OD<sub>600</sub>) were measured using a Shimadzu UV-2450 UV-Vis Spectrophotometer (Shimadzu, Columbia, MD).

S. cerevisiae cultures were grown at 30°C while K. marxianus cultures were grown at 37°C. For luminescence experiments in S. cerevisiae with the Cas6 fusion proteins expressed using the GAL1 promoter, synthetic media SD(-leu) [20 g/L D-glucose (Fisher Scientific), 1.7 g/L yeast nitrogen base without amino acids (BD Difco™), 0.67 g/L CSM-Ura-Leu (Sunrise), 100 mg/L adenine-hemisulfate (Sigma), 100mg/L uracil (Sigma) and 5 g/L ammonium sulfate (Fisher Scientific)] was used for the overnight culture, and SG(-leu) [D-glucose replaced with 20 g/L galactose (Fisher Scientific)] for NanoBiT expression. The cultures were grown for 25-28 h before harvest for the luminescence assay. When Cas6 fusion proteins were expressed using the TEF1 promoter, SD(-leu) was used for both the overnight and the expression cultures. For inducing scaffold expression, cells were grown overnight in SR(-leu) (with 40 g/L raffinose instead of D-glucose) before reinoculation into SR(-leu) to OD 0.1. At 25-28 h, the culture tubes were

centrifuged at 500 rcf for 5 minutes and the supernatant discarded. 3ml of 4% SR(-leu) or 4% SG(-leu) was added and the culture tubes were incubated for either 9 h or 23 h before the luminescence assay. For Violacein expression, cells were cultured in 5ml of SDC (A) [20 g/L D-glucose (Fisher Scientific), 1.7 g/L yeast nitrogen base without amino acids (BD Difco<sup>TM</sup>), 5 g/L Casamino acid (Gibco<sup>TM</sup> Bacto<sup>TM</sup>), 100 mg/L adenine-hemisulfate (Sigma), and 5 g/L ammonium sulfate (Fisher Scientific)] for both the overnight culture and the expression culture. The cells were cultured for 24 h before harvest for HPLC assay.

*K. marxianus* strain CBS712Δ*U*Δ*L* co-transformed with *URA3* and *LEU2*-marked plasmids was cultured in tubes containing synthetic media SD(-ura -leu) [same as 2% SD(-leu) above but without the addition of the 100 mg/L uracil] for the overnight culture, and then reinoculated into SG(-ura -leu) and cultured for 15 h before being the luminescence assay. *K. marxianus* strain CBS712Δ*ULK-Cas6NanoBiT* transformed with a *LEU2*-marked plasmid was cultured overnight in synthetic media SD(-leu) and then reinoculated into SG(-leu) and cultured for 15 h prior to the assay.

# Yeast Transformations

S. cerevisiae strains were cultured overnight at 30 °C in 3 mL of appropriate selection media (or YPD), before reinoculation into fresh media. The samples were allowed to grow for 6 hours before transformation using the Frozen-EZ Yeast Transformation II Kit (Zymo Research, Irvine, CA.) 1 μg of plasmid DNA was used for routine yeast transformation. For CRISR/Cas9 gene integration, the Cas9 plasmid<sup>60</sup> was transformed into the yeast strains first before the strains were cotransformed with 1 μg of gRNA plasmid DNA and 1-2ug of donor DNA. The samples

were plated onto appropriate selective plate and incubated at 30°C for 3-5 days for single colonies to form.

*K. marxianus* strains were transformed using a modified version of the Frozen-EZ Yeast Transformation II Kit (Zymo Research, Irvine, CA). After overnight culture at 30°C in 3 mL of YPD, cells were reinoculated and grown to an  $OD_{600} = 2.0$  before proceeding with the transformation protocol. 10 μL of Sheared Salmon Sperm DNA (Invitrogen) was added prior to the 300-600 ng of plasmid DNA. For CRISPR/Cas9 gene disruptions or integrations, 800 ng of donor DNA was added before the addition of the 300-600 ng of plasmid DNA. The static recovery time was also increased to 1.5 h. For co-transformations, 300 ng of each plasmid was added after 10 μL of Sheared Salmon Sperm DNA, recovery time was increased to 3 h, and instead of plating, cells were resuspended in 3 mL of selective liquid media and grown at 30°C and 250 rpm for 2-3 days. Cultures were then streaked onto selective plates for single colonies.

#### NanoBiT luminescence in S. cerevisiae and K. marxianus

After harvest,  $OD_{600}$  measurements and used to resuspend and normalize all cultures in sterile water to an  $OD_{600} = 10$  for luminescence measurements. Luminescence was assayed using the Nano-Glo® Luciferase Assay System (Promega Corporation, Madison, WI). Briefly,  $50~\mu L$  of each cell culture was transferred to a flat bottom, white 96-well plate and diluted with  $50~\mu L$  water. The Nano-Glo® Luciferase Assay Reagent was prepared by adding Nano-Glo® Luciferase Assay Substrate to the Nano-Glo® Luciferase Assay Buffer 1:50. Once mixed and brought to room temperature,  $100~\mu L$  of the Nano-Glo® Luciferase Assay Reagent was added to each well and mixed by pipetting. Luminescence measurements were recorded using a SpectraMax M3 plate

reader (Molecular Devices, San Jose, CA) over a period of 30 min with an integration time of 500 ms.

# RT-qPCR analysis

Strains BY4741 and BY GALnbit were transformed with p2u-ScrambledBinding and grown following the same growth protocol used for the luminescence assay. Pellets were harvested after 28 h in 2% galactose media, followed by mechanical lysis for total RNA extraction, reverse transcription, and qPCR reactions. Briefly, cell pellets were resuspended in 800 µL of DNA/RNA protection agent supplied with the Monarch® Total RNA Miniprep Kit from NEB and transferred to a screw-top tubes pre-filled with approximately 0.5mL of 0.5mm Zirconia-silicate beads (Fisher Scientific). Cells were subjected to six, 30 second rounds of beating on the FastPrep-24 Classic Bead Beating Grinder and Lysis System (MP Biomedicals, Santa Ana, CA), with 2 minutes spent on ice between rounds. Total RNA extractions from lysed cells were performed following the NEB Monarch® Total RNA Miniprep Kit protocol. cDNA synthesis from extracted RNA samples were performed using the ProtoScript® First Strand cDNA Synthesis Kit from NEB only using the supplied Randomized Primer Mix to allow for reverse transcription of RNAP III-expressed RNA. qPCR reactions were performed using the PowerTrack SYBR Green Master Mix Kit from Applied Biosystems (Thermo Fisher Scientific, Waltham, MA) using an Applied Biosystems® QuantStudio<sup>TM</sup> 7 Flex Real-Time PCR System. Primers for qPCR were designed to bind outside of and amplify the whole Scrambled Binding transcript (Figure S2B). Additional primers were also designed to bind inside the S. cerevisiae ACTI housekeeping gene<sup>62</sup>. Data analyses were performed by normalizing threshold cycles (Ct-values) from experimental groups twice, first

against those from the housekeeping gene ACTI, and then against the WT, using the  $2^{-\Delta\Delta Ct}$  method<sup>63</sup>.

# Extraction and Quantification of Prodeoxyviolacein and Deoxyviolacein

After culturing for 24 h, 5 ml samples were centrifuged at  $2500 \times g$ , the supernatants discarded, and the pellets resuspended in 1 ml methanol. The mixtures were then transferred to glass vials and incubated at  $95^{\circ}$ C for 15 minutes (with occasional mixing via vortex). The mixtures were allowed to cool to room temperature before spinning down at 13,000 g for 5 minutes. The supernatant was removed for HPLC analysis (LC-10Atpumps (Shimadzu), UV–vis detector (SPD-10AVP, Shimadzu), and Zorbax SB-C18 reversed-phase column (2.1\_150mm, Agilent Technologies). Acetic acid-buffered (1%) acetonitrile and water were used as the mobile and aqueous phases, respectively. The samples were run on the HPLC with a gradient program using a 95% to 5% pump B gradient (H<sub>2</sub>O with 1% acetic acid) at a constant flowrate of 0.9 ml/min for 10 minutes. The elution time for prodeoxyviolacein was at 5.3 minutes and deoxyviolacein was at 6.3 minutes.

# **SUPPORTING INFORMATION:**

Gene cassettes of fusion proteins (Figure S1), scaffold constructs used in the study (Figure S2), amount of scaffold transcripts via RT-qPCR (Figure S3), effect of low copy scaffold transcript on specific luminescence (Figure S4), effect of different sugar sources on cell density (Figure S5), specific luminescence at earlier timepoint in inducible scaffold experiment (Figure S6), ratio of desired to total violacein products with limiting Binding Scaffold (Figure S7), schematic of Cas6-

NanoBit fusions in *K. marxianus* (Figure S8), list of strains and plasmids (Table S1), list of primers

(Table S2), and list of gene fragment sequences (Table S3).

**AUTHOR INFORMATION:** 

**Corresponding Author** 

Nancy A. Da Silva – Department of Chemical and Biomolecular Engineering, University of

California, Irvine, CA 92697, United States, Email: ndasilva@uci.edu

**Authors** 

Anhuy Pham - Department of Chemical and Biomolecular Engineering, University of

California, Irvine, CA 92697, United States

Shane Bassett - Department of Chemical and Biomolecular Engineering, University of

California, Irvine, CA 92697, United States

Wilfred Chen - Department of Chemical and Biomolecular Engineering, University of

Delaware, Newark, DE 19716, United States

**Author Contributions** 

N.A.D. and W.C. conceived the project. All authors designed the research; A.P. and S.B.

performed experiments; A.P., S.B., and N.A.D. analyzed data. All authors reviewed and edited the

manuscript.

**CONFLICTS OF INTEREST: None** 

29

# **ACKNOWLEDGEMENTS:**

This research was supported by the National Science Foundation (Grant No. CBET-1803677 and MCB-2013957). We thank Danielle Bever for assistance with RNA extractions, cDNA synthesis, and qPCR.

#### **REFERENCES:**

- (1) Jørgensen, K.; Rasmussen, A. V.; Morant, M.; Nielsen, A. H.; Bjarnholt, N.; Zagrobelny, M.; Bak, S.; Møller, B. L. Metabolon Formation and Metabolic Channeling in the Biosynthesis of Plant Natural Products. *Current Opinion in Plant Biology*. 2005. https://doi.org/10.1016/j.pbi.2005.03.014.
- (2) Agapakis, C. M.; Boyle, P. M.; Silver, P. A. Natural Strategies for the Spatial Optimization of Metabolism in Synthetic Biology. *Nat. Chem. Biol.* 2012 86 **2012**, 8 (6), 527–535. https://doi.org/10.1038/nchembio.975.
- (3) Hammer, S. K.; Avalos, J. L. Harnessing Yeast Organelles for Metabolic Engineering. *Nat. Chem. Biol.* **2017**, *13* (8), 823–832. https://doi.org/10.1038/nchembio.2429.
- (4) Qiu, X. yuan; Xie, S. S.; Min, L.; Wu, X. M.; Zhu, L. Y.; Zhu, L. Spatial Organization of Enzymes to Enhance Synthetic Pathways in Microbial Chassis: A Systematic Review. *Microbial Cell Factories*. 2018. https://doi.org/10.1186/s12934-018-0965-0.
- (5) Meynial Salles, I.; Forchhammer, N.; Croux, C.; Girbal, L.; Soucaille, P. Evolution of a Saccharomyces Cerevisiae Metabolic Pathway in Escherichia Coli. *Metab. Eng.* 2007, 9 (2), 152–159. https://doi.org/10.1016/J.YMBEN.2006.09.002.
- Wang, C.; Yoon, S.-H.; Jang, H.-J.; Chung, Y.-R.; Kim, J.-Y.; Choi, E.-S.; Kim, S.-W. Metabolic Engineering of Escherichia Coli for α-Farnesene Production. *Metab. Eng.* 2011, 13 (6), 648–655. https://doi.org/10.1016/J.YMBEN.2011.08.001.
- (7) Dueber, J. E.; Wu, G. C.; Malmirchegini, G. R.; Moon, T. S.; Petzold, C. J.; Ullal, A. V.; Prather, K. L. J.; Keasling, J. D. Synthetic Protein Scaffolds Provide Modular Control over Metabolic Flux. *Nat. Biotechnol.* **2009**. https://doi.org/10.1038/nbt.1557.
- Wang, Y.; Yu, O. Synthetic Scaffolds Increased Resveratrol Biosynthesis in Engineered Yeast Cells. *J. Biotechnol.* **2012**, *157* (1), 258–260. https://doi.org/10.1016/j.jbiotec.2011.11.003.
- (9) Yang, D.; Park, S. Y.; Park, Y. S.; Eun, H.; Lee, S. Y. Metabolic Engineering of Escherichia Coli for Natural Product Biosynthesis. *Trends Biotechnol.* **2020**, *38* (7), 745–765. https://doi.org/10.1016/j.tibtech.2019.11.007.
- (10) Gad, S.; Ayakar, S. Protein Scaffolds: A Tool for Multi-Enzyme Assembly. *Biotechnol. Reports* **2021**, *32* (September), e00670. https://doi.org/10.1016/j.btre.2021.e00670.
- (11) Siddiqui, M. S.; Thodey, K.; Trenchard, I.; Smolke, C. D. Advancing Secondary Metabolite Biosynthesis in Yeast with Synthetic Biology Tools. *FEMS Yeast Res.* **2012**, *12* (2), 144–170. https://doi.org/10.1111/j.1567-1364.2011.00774.x.

- (12) Yocum, H. C.; Pham, A.; Da Silva, N. A. Successful Enzyme Colocalization Strategies in Yeast for Increased Synthesis of Non-Native Products. *Frontiers in Bioengineering and Biotechnology*. 2021. https://doi.org/10.3389/fbioe.2021.606795.
- (13) Kim, S.; Bae, S. J.; Hahn, J. S. Redirection of Pyruvate Flux toward Desired Metabolic Pathways through Substrate Channeling between Pyruvate Kinase and Pyruvate-Converting Enzymes in Saccharomyces Cerevisiae. *Sci. Rep.* **2016**, *6*. https://doi.org/10.1038/srep24145.
- (14) Lin, J. L.; Zhu, J.; Wheeldon, I. Synthetic Protein Scaffolds for Biosynthetic Pathway Colocalization on Lipid Droplet Membranes. *ACS Synth. Biol.* **2017**. https://doi.org/10.1021/acssynbio.7b00041.
- (15) Tippmann, S.; Anfelt, J.; David, F.; Rand, J. M.; Siewers, V.; Uhlén, M.; Nielsen, J.; Hudson, E. P. Affibody Scaffolds Improve Sesquiterpene Production in Saccharomyces Cerevisiae. *ACS Synth. Biol.* **2017**. https://doi.org/10.1021/acssynbio.6b00109.
- (16) Thodey, K.; Galanie, S.; Smolke, C. D. A Microbial Biomanufacturing Platform for Natural and Semisynthetic Opioids. *Nat. Chem. Biol.* **2014**, *10* (10), 837–844. https://doi.org/10.1038/nchembio.1613.
- (17) Zhao, E. M.; Suek, N.; Wilson, M. Z.; Dine, E.; Pannucci, N. L.; Gitai, Z.; Avalos, J. L.; Toettcher, J. E. Light-Based Control of Metabolic Flux through Assembly of Synthetic Organelles. *Nat. Chem. Biol.* 2019, 15 (6), 589–597. https://doi.org/10.1038/s41589-019-0284-8.
- (18) Lee, H.; DeLoache, W. C.; Dueber, J. E. Spatial Organization of Enzymes for Metabolic Engineering. *Metab. Eng.* **2012**, *14* (3), 242–251. https://doi.org/10.1016/J.YMBEN.2011.09.003.
- (19) Polka, J. K.; Hays, S. G.; Silver, P. A. Building Spatial Synthetic Biology with Compartments, Scaffolds, and Communities. *Cold Spring Harb. Perspect. Biol.* **2016**. https://doi.org/10.1101/cshperspect.a024018.
- (20) Lee, J. H.; Jung, S. C.; Bui, L. M.; Kang, K. H.; Song, J. J.; Kim, S. C. Improved Production of L-Threonine in Escherichia Coli by Use of a DNA Scaffold System. *Appl. Environ. Microbiol.* **2013**, 79 (3), 774–782. https://doi.org/10.1128/AEM.02578-12.
- (21) Liu, Y.; Zhu, Y.; Ma, W.; Shin, H. dong; Li, J.; Liu, L.; Du, G.; Chen, J. Spatial Modulation of Key Pathway Enzymes by DNA-Guided Scaffold System and Respiration Chain Engineering for Improved N-Acetylglucosamine Production by Bacillus Subtilis. *Metab. Eng.* **2014**, *24*, 61–69. https://doi.org/10.1016/j.ymben.2014.04.004.
- (22) Xie, S. si; Qiu, X. yuan; Zhu, L. yun; Zhu, C. shu; Liu, C. yang; Wu, X. min; Zhu, L.; Zhang, D. yi. Assembly of TALE-Based DNA Scaffold for the Enhancement of Exogenous

- Multi-Enzymatic Pathway. *J. Biotechnol.* **2019**, *296*, 69–74. https://doi.org/10.1016/j.jbiotec.2019.03.008.
- (23) Berckman, E. A.; Chen, W. Exploiting DCas9 Fusion Proteins for Dynamic Assembly of Synthetic Metabolons. *Chem. Commun.* **2019**. https://doi.org/10.1039/c9cc04002a.
- (24) Niewoehner, O.; Jinek, M.; Doudna, J. A. Evolution of CRISPR RNA Recognition and Processing by Cas6 Endonucleases. *Nucleic Acids Res.* **2014**. https://doi.org/10.1093/nar/gkt922.
- (25) Conrado, R. J.; Wu, G. C.; Boock, J. T.; Xu, H.; Chen, S. Y.; Lebar, T.; Turnek, J.; Tomšič, N.; Avbelj, M.; Gaber, R.; Koprivnjak, T.; Mori, J.; Glavnik, V.; Vovk, I.; Beninča, M.; Hodnik, V.; Anderluh, G.; Dueber, J. E.; Jerala, R.; Delisa, M. P. DNA-Guided Assembly of Biosynthetic Pathways Promotes Improved Catalytic Efficiency. *Nucleic Acids Res.* **2012**. https://doi.org/10.1093/nar/gkr888.
- (26) Delebecque, C. J.; Lindner, A. B.; Silver, P. A.; Aldaye, F. A. Organization of Intracellular Reactions with Rationally Designed RNA Assemblies. *Science* (80-. ). **2011**. https://doi.org/10.1126/science.1206938.
- (27) Sachdeva, G.; Garg, A.; Godding, D.; Way, J. C.; Silver, P. A. In Vivo Co-Localization of Enzymes on RNA Scaffolds Increases Metabolic Production in a Geometrically Dependent Manner. *Nucleic Acids Res.* **2014**, *42* (14), 9493–9503. https://doi.org/10.1093/nar/gku617.
- (28) Šulc, P.; Ouldridge, T. E.; Romano, F.; Doye, J. P. K.; Louis, A. A. Modelling Toehold-Mediated RNA Strand Displacement. *Biophys. J.* **2015**, *108* (5), 1238–1247. https://doi.org/10.1016/j.bpj.2015.01.023.
- (29) Siu, K. H.; Chen, W. Riboregulated Toehold-Gated GRNA for Programmable CRISPR—Cas9 Function. *Nat. Chem. Biol.* 2018 153 **2018**, 15 (3), 217–220. https://doi.org/10.1038/s41589-018-0186-1.
- (30) Carte, J.; Pfister, N. T.; Compton, M. M.; Terns, R. M.; Terns, M. P. Binding and Cleavage of CRISPR RNA by Cas6. *RNA* **2010**, *16* (11), 2181–2188. https://doi.org/10.1261/rna.2230110.
- (31) Haurwitz, R. E.; Sternberg, S. H.; Doudna, J. A. Csy4 Relies on an Unusual Catalytic Dyad to Position and Cleave CRISPR RNA. *EMBO J.* **2012**. https://doi.org/10.1038/emboj.2012.107.
- (32) Hochstrasser, M. L.; Doudna, J. A. Cutting It Close: CRISPR-Associated Endoribonuclease Structure and Function. *Trends in Biochemical Sciences*. 2015. https://doi.org/10.1016/j.tibs.2014.10.007.
- (33) Mitkas, A. A.; Valverde, M.; Chen, W. Dynamic Modulation of Enzyme Activity by

- Synthetic CRISPR-Cas6 Endonucleases. *Nat. Chem. Biol.* **2022**, *18* (5), 492–500. https://doi.org/10.1038/s41589-022-01005-7.
- (34) Brouns; JJ, S.; Jore, M. M.; Lundgren, M.; Westra, E. R.; Slijkhuis, R. J.; Snijders, A. P.; Dickman, M. J.; Makarova, K. S.; Koonin, E. V.; Oost, J. Van Der. Small CRISPR RNAs Guide Antiviral Defense in Prokaryotes. *Science* (80-.). 2008.
- (35) Hall, M. P.; Unch, J.; Binkowski, B. F.; Valley, M. P.; Butler, B. L.; Wood, M. G.; Otto, P.; Zimmerman, K.; Vidugiris, G.; Machleidt, T.; Robers, M. B.; Benink, H. A.; Eggers, C. T.; Slater, M. R.; Meisenheimer, P. L.; Klaubert, D. H.; Fan, F.; Encell, L. P.; Wood, K. V. Engineered Luciferase Reporter from a Deep Sea Shrimp Utilizing a Novel Imidazopyrazinone Substrate. *ACS Chem. Biol.* **2012**, *7* (11), 1848–1857. https://doi.org/10.1021/cb3002478.
- (36) Dixon, A. S.; Schwinn, M. K.; Hall, M. P.; Zimmerman, K.; Otto, P.; Lubben, T. H.; Butler, B. L.; Binkowski, B. F.; MacHleidt, T.; Kirkland, T. A.; Wood, M. G.; Eggers, C. T.; Encell, L. P.; Wood, K. V. NanoLuc Complementation Reporter Optimized for Accurate Measurement of Protein Interactions in Cells. ACS Chem. Biol. 2016. https://doi.org/10.1021/acschembio.5b00753.
- (37) Mikkelsen, M. D.; Buron, L. D.; Salomonsen, B.; Olsen, C. E.; Hansen, B. G.; Mortensen, U. H.; Halkier, B. A. Microbial Production of Indolylglucosinolate through Engineering of a Multi-Gene Pathway in a Versatile Yeast Expression Platform. *Metab. Eng.* **2012**. https://doi.org/10.1016/j.ymben.2012.01.006.
- (38) Lee, M. E.; DeLoache, W. C.; Cervantes, B.; Dueber, J. E. A Highly Characterized Yeast Toolkit for Modular, Multipart Assembly. *ACS Synth. Biol.* **2015**. https://doi.org/10.1021/sb500366v.
- (39) Partow, S.; Siewers, V.; Bjørn, S.; Nielsen, J.; Maury, J. Characterization of Different Promoters for Designing a New Expression Vector in Saccharomyces Cerevisiae. *Yeast* **2010**, *27* (11). https://doi.org/10.1002/yea.1806.
- (40) Peng, B.; Williams, T. C.; Henry, M.; Nielsen, L. K.; Vickers, C. E. Controlling Heterologous Gene Expression in Yeast Cell Factories on Different Carbon Substrates and across the Diauxic Shift: A Comparison of Yeast Promoter Activities. *Microb. Cell Fact.* **2015**, *14* (1). https://doi.org/10.1186/s12934-015-0278-5.
- (41) Jakočiūnas, T.; Bonde, I.; Herrgård, M.; Harrison, S. J.; Kristensen, M.; Pedersen, L. E.; Jensen, M. K.; Keasling, J. D. Multiplex Metabolic Pathway Engineering Using CRISPR/Cas9 in Saccharomyces Cerevisiae. *Metab. Eng.* **2015**, *28*, 213–222. https://doi.org/10.1016/J.YMBEN.2015.01.008.
- (42) Deaner, M.; Mejia, J.; Alper, H. S. Enabling Graded and Large-Scale Multiplex of Desired

- Genes Using a Dual-Mode DCas9 Activator in Saccharomyces Cerevisiae. *ACS Synth. Biol.* **2017**. https://doi.org/10.1021/acssynbio.7b00163.
- (43) Raschmanová, H.; Weninger, A.; Glieder, A.; Kovar, K.; Vogl, T. Implementing CRISPR-Cas Technologies in Conventional and Non-Conventional Yeasts: Current State and Future Prospects. *Biotechnol. Adv.* **2018**, *36* (3), 641–665. https://doi.org/10.1016/J.BIOTECHADV.2018.01.006.
- (44) Lee, M. E.; Aswani, A.; Han, A. S.; Tomlin, C. J.; Dueber, J. E. Expression-Level Optimization of a Multi-Enzyme Pathway in the Absence of a High-Throughput Assay. *Nucleic Acids Res.* **2013**. https://doi.org/10.1093/nar/gkt809.
- (45) Loison, G.; Vidal, A.; Findeli, A.; Roitsch, C.; Balloul, J. M.; Lemoine, Y. High Level of Expression of a Protective Antigen of Schistosomes in Saccharomyces Cerevisiae. *Yeast* **1989**, *5* (6). https://doi.org/10.1002/yea.320050609.
- (46) Romanos, M. A.; Scorer, C. A.; Clare, J. J. Foreign Gene Expression in Yeast: A Review. *Yeast* **1992**, *8* (6). https://doi.org/10.1002/yea.320080602.
- (47) Bao, Z.; Xiao, H.; Liang, J.; Zhang, L.; Xiong, X.; Sun, N.; Si, T.; Zhao, H. Homology-Integrated CRISPR-Cas (HI-CRISPR) System for One-Step Multigene Disruption in Saccharomyces Cerevisiae. *ACS Synth. Biol.* **2015**. https://doi.org/10.1021/sb500255k.
- (48) Lane, M. M.; Morrissey, J. P. Kluyveromyces Marxianus: A Yeast Emerging from Its Sister's Shadow. *Fungal Biol. Rev.* **2010**, 24 (1–2), 17–26. https://doi.org/10.1016/j.fbr.2010.01.001.
- (49) Karim, A.; Gerliani, N.; Aïder, M. Kluyveromyces Marxianus: An Emerging Yeast Cell Factory for Applications in Food and Biotechnology. *International Journal of Food Microbiology*. 2020. https://doi.org/10.1016/j.ijfoodmicro.2020.108818.
- (50) Groeneveld, P.; Stouthamer, A. H.; Westerhoff, H. V. Super Life How and Why "cell Selection" Leads to the Fastest-Growing Eukaryote. *FEBS J.* **2009**. https://doi.org/10.1111/j.1742-4658.2008.06778.x.
- (51) McTaggart, T. L.; Bever, D.; Bassett, S.; Da Silva, N. A. Synthesis of Polyketides from Low Cost Substrates by the Thermotolerant Yeast Kluyveromyces Marxianus . *Biotechnol. Bioeng.* **2019**. https://doi.org/10.1002/bit.26976.
- (52) Nonklang, S.; Abdel-Banat, B. M. A.; Cha-aim, K.; Moonjai, N.; Hoshida, H.; Limtong, S.; Yamada, M.; Akada, R. High-Temperature Ethanol Fermentation and Transformation with Linear DNA in the Thermotolerant Yeast Kluyveromyces Marxianus DMKU3-1042. *Appl. Environ. Microbiol.* **2008**. https://doi.org/10.1128/AEM.01854-08.
- (53) Urit, T.; Li, M.; Bley, T.; Löser, C. Growth of Kluyveromyces Marxianus and Formation

- of Ethyl Acetate Depending on Temperature. *Appl. Microbiol. Biotechnol.* **2013**. https://doi.org/10.1007/s00253-013-5278-y.
- (54) Liu, Z.; Chen, O.; Wall, J. B. J.; Zheng, M.; Zhou, Y.; Wang, L.; Ruth Vaseghi, H.; Qian, L.; Liu, J. Systematic Comparison of 2A Peptides for Cloning Multi-Genes in a Polycistronic Vector. *Sci. Rep.* **2017**. https://doi.org/10.1038/s41598-017-02460-2.
- (55) Bever, D.; Wheeldon, I.; Da Silva, N. RNA Polymerase II-Driven CRISPR-Cas9 System for Efficient Non-Growth-Biased Metabolic Engineering of Kluyveromyces Marxianus. *Metab. Eng. Commun.* **2022**, e00208. https://doi.org/https://doi.org/10.1016/j.mec.2022.e00208.
- (56) Souza-Moreira, T. M.; Navarrete, C.; Chen, X.; Zanelli, C. F.; Valentini, S. R.; Furlan, M.; Nielsen, J.; Krivoruchko, A. Screening of 2A Peptides for Polycistronic Gene Expression in Yeast. *FEMS Yeast Res.* **2018**. https://doi.org/10.1093/femsyr/foy036.
- (57) Zadeh, J. N.; Steenberg, C. D.; Bois, J. S.; Wolfe, B. R.; Pierce, M. B.; Khan, A. R.; Dirks, R. M.; Pierce, N. A. NUPACK: Analysis and Design of Nucleic Acid Systems. *J. Comput. Chem.* 2011. https://doi.org/10.1002/jcc.21596.
- (58) Siu, K.-H. SYNTHETIC BIOMOLECULAR CONTROL SYSTEMS TO REPROGRAM CELLULAR FUNCTIONS AND DYNAMIC RESPONSES, University of Delaware, 2019.
- (59) Besada-Lombana, P. B.; Da Silva, N. A. Engineering the Early Secretory Pathway for Increased Protein Secretion in Saccharomyces Cerevisiae. *Metab. Eng.* **2019**, *55* (May), 142–151. https://doi.org/10.1016/j.ymben.2019.06.010.
- (60) Yocum, H. C. Enhancing Polyketide Production in Yeast via Increased Access to Acetyl-CoA Pools, University of California, Irvine, 2021.
- (61) Rajkumar, A. S.; Varela, J. A.; Juergens, H.; Daran, J. M. G.; Morrissey, J. P. Biological Parts for Kluyveromyces Marxianus Synthetic Biology. *Front. Bioeng. Biotechnol.* **2019**. https://doi.org/10.3389/fbioe.2019.00097.
- (62) Teste, M. A.; Duquenne, M.; François, J. M.; Parrou, J. L. Validation of Reference Genes for Quantitative Expression Analysis by Real-Time RT-PCR in Saccharomyces Cerevisiae. *BMC Mol. Biol.* **2009**. https://doi.org/10.1186/1471-2199-10-99.
- (63) Livak, K. J.; Schmittgen, T. D. Analysis of Relative Gene Expression Data Using Real-Time Quantitative PCR and the 2-ΔΔCT Method. *Methods* **2001**. https://doi.org/10.1006/meth.2001.1262.

# **Table of Contents Figure**

